Acta Crystallographica Section D
Biological Crystallography
ISSN 0907-4449

Crystallization and preliminary X-ray study of an N-terminal fragment of rat liver ribosomal P2 protein

David Mandelman,[a]† Philippe Gonzalo,[b]† Jean-Pierre Lavergne,[b] Catherine Corbier,[c] Jean-Paul Reboud[b] and Richard Haser[a]*

[a]Laboratoire de Bio-Cristallographie, Institut de Biologie et Chimie des Protéines, CNRS et Université Claude Bernard Lyon I–UMR 5086, 69367 Lyon CEDEX 07, France, [b]Laboratoire de Biologie Médicale, Institut de Biologie et Chimie des Protéines, CNRS et Université Claude Bernard Lyon I–UMR 5086, 69367 Lyon CEDEX 07, France, and [c]Laboratoire de Cristallographie et Modélisation des Matériaux Minéraux et Biologiques, CNRS–UPRESA 7036, Université Henri Poincaré–Nancy I, Boulevard des Aiguillettes, 54506 Vandoeuvre-lès-Nancy CEDEX, France

† These authors made equal contributions.

Correspondence e-mail: r.haser@ibcp.fr

Received 18 October 2001
Accepted 30 January 2002

Ribosomal P proteins have been shown to be involved in the binding of elongation factors and participate in factor-dependent GTP hydrolysis. The P proteins form the pentamer $(P1/P2)_2$–P0 constituting the lateral flexible stalk of the 60S ribosomal subunit. The highly soluble domain (1–65) of rat liver P2 has been overexpressed in *Escherichia coli* as an N-terminal poly-His-tagged protein and crystallized. To reduce nucleation and improve crystal morphology and diffraction power, the crystals were grown in a gel matrix and an oil barrier was added between the reservoir and the drop to reduce the rate of vapour diffusion. This dramatically reduced the nucleation in the drops and yielded diffraction-quality crystals. Data were collected to 2.4 Å resolution at beamline ID 14-1, ESRF. The crystals belong to the orthorhombic space group $P2_12_12$, with unit-cell parameters a = 37.7, b = 96.7, c = 135.0 Å.

1. Introduction

Eukaryotic ribosomes are large ribonucleoprotein complexes of about 4.5 MDa responsible for the accurate translation of the genetic material into proteins (Pestka, 1968; Ibba & Soll, 1999). The P proteins P0, P1 and P2 constitute the flexible lateral stalk of the large subunit that is connected to a small portion of the 28S rRNA (nucleotides 1850–1930) designated as the thiostreptone loop or the GTPase centre. In the stalk, P1 and P2 (11.5 kDa) are very acidic proteins each found as two copies in connection with a single copy of P0 (34.2 kDa). P0 is bound directly to the GTPase centre and to a sixth protein, L12, that is also bound to the GTPase centre (Uchiumi & Kominami, 1992). The P proteins have been found to be essential for effective proteosynthetic activity (MacConnell & Kaplan, 1980; Vard *et al.*, 1997). They are part of the translation-factor binding site and are involved in the GTP-hydrolysis activation of these translational factors (Bargis-Surgey *et al.*, 1999). The P proteins belong to the few phosphorylable and phosphorylated proteins of the ribosome (Hasler *et al.*, 1991). P2 is the most phosphorylated member of this group, probably owing to the organization of the stalk, which places it in a protruding situation, and its phosphorylation has previously been shown to be crucial for the translational activity of the ribosome (Gonzalo *et al.*, 2001; Vard *et al.*, 1997). Since both P1 and P2 are in rapid exchange between a ribosomal pool and a cytoplasmic pool, a sophisticated mode of regulation of the elongation step of protein synthesis might occur through this protein (Zinker & Warner, 1976; Mitsui *et al.*, 1988; Tsurugi & Ogata, 1985).

Recently, medium- to high-resolution X-ray crystal structures of small and large prokaryotic ribosomal particles as well as a complete intact 70S ribosome (Yusupov *et al.*, 2001) have been elucidated and reveal a fairly complex organization of an rRNA core with a protein-rich periphery. In the 2.4 Å high-resolution structure of the large ribosomal subunit (Ban *et al.*, 2000), 27 protein structures were identified along with 2833 nucleotides in the complete particle. Unfortunately, the flexible lateral stalk made up of the proteins L7/L12 and involved in peptide elongation was left unidentified owing to a lack of clear electron density. The absence of good electron density in this area of the ribosome is in part a consequence of the fact that the lateral stalk is extremely mobile, as shown in low-resolution maps obtained by cryo-electron microscopy (Gabashvili *et al.*, 2000) and cross-linking experiments (Oleinikov *et al.*, 1993). The initial structure of L12 alone was solved by MAD methods (Wahl, Bourenkov *et al.*, 2000) and provided a model for homodimerization of L12 in the stalk region. The structure of L7/L12 was subsequently revealed in the 3.1 Å structure of the large subunit from *Deinococcus radiodurans* (Harms *et al.*, 2001) and in the 5.5 Å structure of the 70S ribosome (Yusupov *et al.*, 2001), with both stalks adopting different orientations relative to the ribosome and to each other. A third orientation of the L7/L12 protuberance has been observed in a structure in which only the rRNA portion of this region was resolved (PDB code 1jj2). These three

© 2002 International Union of Crystallography
Printed in Denmark – all rights reserved

conformations of the L7/L12 stalk further testify to the flexibility associated with the translocation step carried out following binding of various elongation factors. Additional structural details of the ribosome include the large ribosomal subunit of *D. radiodurans* complexed with medically relevant antibiotics (Schlunzen *et al.*, 2001) and provides insight into ribosome–drug interaction, thus opening the door for rational drug design.

Trials to obtain crystals using full-length P1 or P2 were unsuccessful, probably owing to the intrinsic flexibility of these proteins. More precisely, an alanine/proline-rich domain at the C-terminus of these proteins would account for the ability of these proteins to undergo large conformational changes. The crystallographic structure for full-length L7/L12, the counterpart of the P1 and P2 proteins (Wahl, Huber *et al.*, 2000) is unlikely to be similar to that of P1 and P2, since L7/L12 and P1 or P2 are very different proteins. Indeed, although they are of similar length (about 110 residues), L7/L12 and P1/P2 share no sequence homology except for the presence of the intermediary flexible region (Szick *et al.*, 1998). However, in P1/P2 the N-terminal domain is large (approximately 65 residues), whereas it is quite small in L7/L12. The C-terminal domain that is protruding is short (20 residues), charged and contains two phosphorylation sites on serine residues (Hasler *et al.*, 1991). In addition, in contrast to L7 and L12, which differ only by the acetylation of the N-terminus in L7 (Terhorst *et al.*, 1973), P1 and P2 have very different sequences in their N-terminal domain and have been demonstrated to play different roles in protein synthesis (Wool *et al.*, 1991; Vard *et al.*, 1997). Indeed, in recently published results we have obtained a model of the organization of the P proteins in the lateral stalk (Gonzalo *et al.*, 2001). In this model, the N-terminal domain of P1 constitutes a bridge that attaches P2 to P0. Determination of the structure of N2 will be of tremendous interest in better understanding the structural background that supports the interactions and motility of P proteins.

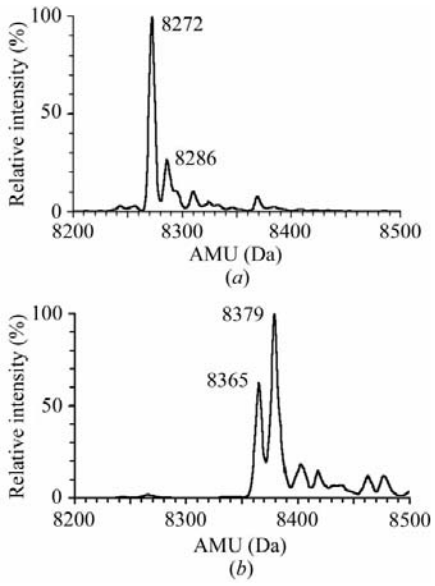

Figure 1
Electrospray mass spectrum of (*a*) native and (*b*) SeMet-substituted N2 protein. The graphs have been normalized to the tallest peak in the spectrum. The molecular masses (AMU) represent an averaging of the various charged states of the ionized species (*m*/*z*).

2. Methods and materials

2.1. Expression, purification and crystallization

The cloning and expression of the truncated mutant of P2, N2 (residues 1–65 of P2), has already been described elsewhere (Gonzalo *et al.*, 2001). For the SeMet-substituted protein an identical bacterial expression system was used, but high concentrations of the amino acids Lys, Phe, Thr, L-selenomethionine (200 mg l^{-1}), Ile, Leu and Val (100 mg l^{-1}) were added to a minimal media culture at mid-log phase to inhibit the natural methionine pathway of the bacteria (Doublie, 1997). Selenomethionine substitution was verified with an Applied Biosystems (API-165) electrospray mass spectrometer (Fig. 1). The sample was diluted in 50% methanol, 0.1% formic acid.

The purified proteins were dialyzed against 50 m*M* Tris–HCl pH 7.4, 20 m*M* KCl, 10%(*w*/*v*) glycerol, 4 m*M* 2-mercaptoethanol and frozen at 193 K. Crystallization conditions were sought using the His-tagged native protein at 23 mg ml^{-1} by the hanging-drop vapour-diffusion method (McPherson, 1999).

Initial N2 crystallization conditions in PEG 600 yielded small hexagonal crystals that were non-isomorphous. Subsequent screening in higher molecular weight PEGs in combination with additive screening (Hampton Research, USA; Jancarik & Kim, 1991) produced a new crystal morphology. The addition of 1.5% 1,2,3-heptanetriol (HT) to 33% PEG 2000 MME successfully produced a shower of small needle crystals at 290 K. The problem then arose of reducing the amount of nucleation in order to produce larger crystals. The technique of crystallization in a gel matrix (Cudney *et al.*, 1994) was used to reduce the amount of spontaneous nucleation in the drop and improve the crystal quality. The nucleation was reduced and the crystal size increased, but the crystals grew too rapidly and showed signs of cracking after a few days. To overcome this problem, the crystallization temperature was reduced to 277 K and an oil barrier (Chayen, 1997) was added to the reservoir to reduce the rate of vapour diffusion in the well. Crystallization was noticeably slowed and the number of nuclei in the drop was dramatically reduced. Concomitant with this observation was a noticeable increase in crystal size without the cracking observed at 290 K. The crystals grew to full size in 3–4 weeks, forming hexagonal rods (Fig. 2).

2.2. Data collection and processing

When the crystals attained their maximum size, X-ray diffraction experiments were conducted under cryogenic conditions. The crystals were disentangled from their agarose-gel matrix in 1.5% HT, 40% PEG 2000 MME, a PEG concentration suitable for cryoprotection (Garman & Schneider, 1997). The hexagonal rod crystals

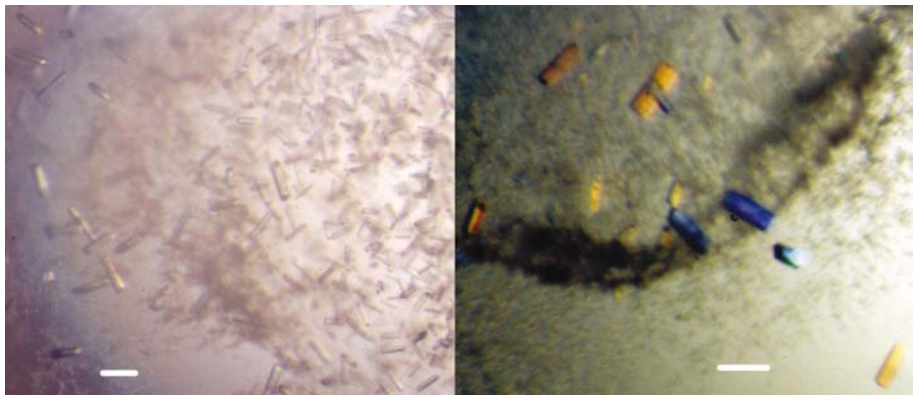

Figure 2
Crystals of the N-terminal fragment of rat liver P2 protein. The white scale bars indicate 100 µm.

diffracted to 3.1 Å on an in-house Cu-anode generator and the resolution was extended to 2.4 Å (Fig. 3, Table 1) through the use of synchrotron radiation at beamline ID 14-1 of the European Synchrotron Radiation Facility (ESRF, Grenoble, France). The data were indexed and integrated with *MOSFLM* (Leslie, 1987) and reduced with *SCALA* in collaboration with other *CCP*4 programs (Collaborative Computational Project, Number 4, 1994). The crystal mosaicity was refined to 0.9°, which could in part be a consequence of the lack of proper cryoprotection, but is more likely to arise from the physical manipulations required to extract the crystals from their agarose-gel matrix. The crystals belong to the orthorhombic space group $P2_12_12$, with the unit-cell parameters given in Table 1. Currently, the space group $P222_1$ is also being considered owing to the existence of a strong reflection at 900 with an $I/\sigma(I)$ of 16. This reflection is recurrent throughout other N2 diffraction data sets collected and may eliminate the screw axis along *a*. This space-group ambiguity will be resolved during phase determination.

The Matthews coefficient (V_M) (Matthews, 1968) was calculated to estimate the number of molecules and the solvent content of the asymmetric unit (Table 1). Between six and eight molecules are expected in the asymmetric unit.

Table 1
X-ray diffraction data.

Values in parentheses are for the highest resolution shell.

Space group	$P2_12_12$		
Unit-cell parameters (Å, °)	a = 37.7, b = 96.7, c = 135.0, $\alpha = \beta = \gamma$ = 90		
No. of observed reflections	107016		
No. of unique reflections	19837		
Redundancy	5.4		
Resolution range (Å)	36.0–2.4 (2.46–2.40)		
$I/\sigma(I)$	8.1 (2.0)		
Completeness (%)	98.6 (98.6)		
R_{sym} (%)	7.9 (35.0)		
Mosaicity (°)	0.9		
No. of molecules per AU	6	7	8
V_M (Å^3 Da^{-1})	2.6	2.2	1.9
Solvent content (%)	53	44	35

† $R_{sym}(I) = \sum |I_n - \langle I \rangle| / \sum I_n$.

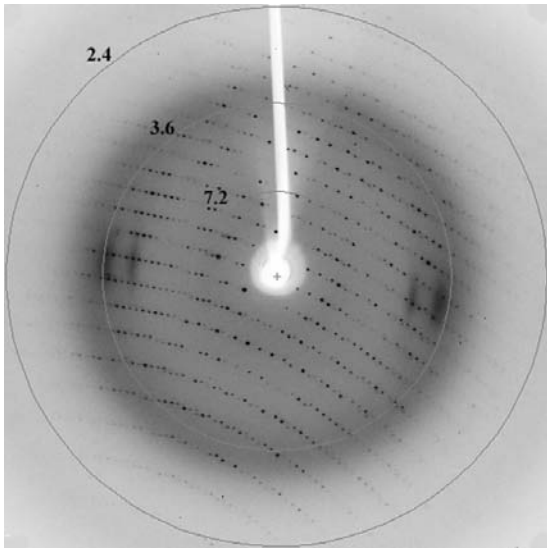

Figure 3
A 1° oscillation image collected from an N2 crystal at beamline ID 14-1, ESRF at 100 K.

3. Discussion

A substantial step forward has been achieved for the crystallization and eventual structure solution of the N-terminal domain of the mammalian acidic ribosomal protein P2. The initial crystallization of full-length P2 gave no crystals. To overcome this problem, the protein was truncated to residues 1–65, a region of the protein currently hypothesized to participate in homodimerization (Gonzalo *et al.*, 2001). Initial crystallization trials in low-molecular-weight PEG (PEG 600) without additives gave hexagonal crystals that diffracted, but indexing of the *c* axis was indeterminate. The addition of the alcohol 1,2,3-heptanetriol (HT) to PEG 2000 along with techniques to slow crystal nucleation and growth produced diffraction-quality crystals that are reproducibly isomorphous. It is likely that the HT affects the monomer–dimer equilibrium, forcing the protein into a more homogenous state. Currently, this hypothesis has not been tested biochemically.

In order to phase the protein using the multi-wavelength anomalous dispersion (MAD) technique, selenomethionine-substituted N2 has been expressed and purified and crystallization experiments are under way. Complete substitution of the methionine S atoms by selenium was verified by electrospray ionization mass spectrometry (ES/MS; Fig. 1). The difference in molecular weight between the two ionized species corresponds to the molecular weight of two Se atoms and is in agreement with the expected sequence of N2. A second protein species differing by 14 Da exists in the mass spectrum of N2 and might be explained by the methylation of a residue such as a lysine; the solved P2 structure will resolve this issue. In any case, both species were completely substituted with selenomethionine. The SeMet protein exhibited reduced solubility as previously described for other proteins (Doublie, 1997), but could still be concentrated to 25 mg ml^{-1} for crystallization trials. The parameters around the native N2 crystallization have been tested and small crystals have begun to appear.

We thank Hassan Belrhali for his help at beamline ID 14-1 of the European Synchrotron Radiation Facility (ESRF) in Grenoble, France. We would also like to thank Michel Becchi for his expertise in the mass spectrometric analysis of the selenomethionine-substituted N2 protein. This work was supported in part by the Fondation Pour La Recherche Medicale (FRM) and the Hospices Civils de Lyon.

References

Ban, N., Nissen, P., Hansen, J., Moore, P. B. & Steitz, T. A. (2000). *Science*, **289**, 905–920.
Bargis-Surgey, P., Lavergne, J. P., Gonzalo, P., Vard, C., Filhol-Cochet, O. & Reboud, J. P. (1999). *Eur. J. Biochem.* **262**, 606–611.
Chayen, N. E. (1997). *J. Appl. Cryst.* **30**, 198–202.
Collaborative Computational Project, Number 4 (1994). *Acta Cryst.* D**50**, 760–763.
Cudney, R., Patel, S. & McPherson, A. (1994). *Acta Cryst.* D**50**, 479–483.
Doublie, S. (1997). *Methods Enzymol.* **276**, 523–530.
Gabashvili, I. S., Agrawal, R. K., Spahn, C. M., Grassucci, R. A., Svergun, D. I., Frank, J. & Penczek, P. (2000). *Cell*, **100**, 537–549.
Garman, E. F. & Schneider, T. R. (1997). *J. Appl. Cryst.* **30**, 211–237.
Gonzalo, P., Lavergne, J. P. & Reboud, J. P. (2001). *J. Biol. Chem.* **276**, 19762–19769.
Harms, J., Schluenzen, F., Zarivach, R., Bashan, A., Gat, S., Agmon, I., Bartels, H., Franceschi, F. & Yonath, A. (2001). *Cell*, **107**, 679–688.
Hasler, P., Brot, N., Weissbach, H., Parnassa, A. P. & Elkon, K. B. (1991). *J. Biol. Chem.* **266**, 13815–13820.
Ibba, M. & Soll, D. (1999). *Science*, **286**, 1893–1897.
Jancarik, J. & Kim, S.-H. (1991). *J. Appl. Cryst.* **24**, 409–411.
Leslie, A. G. W. (1987). *Proceedings of the Daresbury Study Weekend. Computational Aspects of Protein Crystal Data Analysis*, edited by J. R. Helliwell, P. A. Machin & M. Z. Papiz, pp. 39–50. Warrington: Daresbury Laboratory.
MacConnell, W. P. & Kaplan, N. O. (1980). *Biochem. Biophys. Res. Commun.* **92**, 46–52.
McPherson, A. (1999). *Crystallization of Biological Macromolecules.* New York: Cold Spring Harbor Laboratory Press.
Matthews, B. W. (1968). *J. Mol. Biol.* **33**, 491–497.
Mitsui, K., Nakagawa, T. & Tsurugi, K. (1988). *J. Biochem. (Tokyo)*, **104**, 908–911.
Oleinikov, A. V., Jokhadze, G. G. & Traut, R. R. (1993). *Proc. Natl Acad. Sci. USA*, **90**, 9828–9831.
Pestka, S. (1968). *J. Biol. Chem.* **243**, 2810–2820.

Schlunzen, F., Zarivach, R., Harms, J., Bashan, A., Tocilj, A., Albrecht, R., Yonath, A. & Franceschi, F. (2001). *Nature (London)*, **413**, 814–821.
Szick, K., Springer, M. & Bailey-Serres, J. (1998). *Proc. Natl Acad. Sci. USA*, **95**, 2378–2383.
Terhorst, C., Moller, W., Laursen, R. & Wittmann-Liebold, B. (1973). *Eur. J. Biochem.* **34**, 138–152.
Tsurugi, K. & Ogata, K. (1985). *J. Biochem. (Tokyo)*, **98**, 142714–142731.
Uchiumi, T. & Kominami, R. (1992). *J. Biol. Chem.* **267**, 19179–19185.
Vard, C., Guillot, D., Bargis, P., Lavergne, J. P. & Reboud, J. P. (1997). *J. Biol. Chem.* **272**, 20259–20262.
Wahl, M. C., Bourenkov, G. P., Bartunik, H. D. & Huber, R. (2000). *EMBO J.* **19**, 174–186.
Wahl, M. C., Huber, R., Marinkovic, S., Weyher-Stingl, E. & Ehlert, S. (2000). *J. Biol. Chem.* **381**, 221–229.
Wool, I. G., Chan, Y. L., Gluck, A. & Suzuki, K. (1991). *Biochimie*, **73**, 861–870.
Yusupov, M. M., Yusupova, G. Z., Baucom, A., Lieberman, K., Earnest, T. N., Cate, J. H. & Noller, H. F. (2001). *Science*, **292**, 883–896.
Zinker, S. & Warner, J. R. (1976). *J. Biol. Chem.* **251**, 1799–1807.